World Conference on Timber Engineering Oslo 2023

SIMULATION OF WOOD FRACTURE MECHANICS USING THE PHASE FIELD METHOD FOR FRACTURE

Sebastian Pech[1], Markus Lukacevic[2], Josef Füssl[3]

ABSTRACT: Fracture mechanics simulations play a crucial role in predicting the failure of materials in various engineering applications. However, modeling fracture in inhomogeneous materials with complex microstructures is challenging. This work applies a non-brittle hybrid multi-phase field model to simulate wood failure. The approach is based on a stress-based split for orthotropic materials and includes multiple phase field variables, incorporating preferable fracture planes. The proposed model is initially applied to two examples, single-edge notched plates with varying fiber inclines and a wooden board with a single knot and spatially varying fiber directions. Both examples show that the model covers the effect of the wood microstructure on macroscopic crack propagation. Subsequently, the model is validated on experimental studies from the literature. We show that by choosing the input parameters, the tensile strength and the fracture energy release rate, in a reasonable range for wood, the model agrees well with the results of the experimental studies. Those findings open the application of the model to more complex situations like wooden boards with multiple knots and show that the used input parameters are not model-specific numerically tuned parameters but rather material-specific quantities.

KEYWORDS: Fracture, phase field method, wood

1 INTRODUCTION

Wood is consequently gaining importance in fields of civil engineering, where mainly steel and concrete constructions have dominated until now. This uprise is primarily due to new developments of high-performance wood-based products, the rediscovery of the excellent performance of wood as a building material and ecological benefits.

Understanding the complex mechanical nature of wood is critical to opening its application in new fields and optimizing its usage.

The microstructure of wood strongly influences its mechanical properties. Crack growth starts on the microscopic scale from defects in the cell wall material. After the localization of a macroscopic crack, a fracture process zone forms [31]. Subsequently, toughening effects like fiber bridging [11,35] set in. Microcracks and toughening effects result in a cohesive material behavior. The microstructure also strongly influences the macroscopic crack orientation. Wood fibers, which were produced at the same time, lie on so-called growth surfaces. Such growth surfaces give structure to the material. With a weak interface between the fibers, cracks tend to follow the direction of least resistance along the fiber [31]. Together with a spatially strongly varying fiber orientation, macroscopic crack topologies become very complex. In summary, for simulating wood fracture, a numerical method is required capable of accounting for an orthotropic constitutive behavior, cohesive fracture, preferable fracture planes, and complex three-dimensional cracks.

At the Institute for Mechanics of Materials and Structures (IMWS), we followed two quite promising methods in recent years: Finite element-based limit analysis [19] and the extended finite element method (XFEM) [21,24]. Both approaches show a good but not yet satisfying performance. Particularly the latter approach suffers geometrical limitations which do not allow for modeling the complex crack paths found in wood fracture.

A method well suited for crack paths of arbitrary complexity is the phase field method for fracture [4,5,12,23]. It is based on Griffith's theory of brittle fracture [13], formulated by a variational approach, minimizing the total energy of the system. An auxiliary field $d \in [0,1]$ models cracks, including a smooth transition between the intact ($d = 0$) and the cracked ($d = 1$) solid.

The original phase field method cannot account for wood fracture phenomena. In particular, the formulation does not include orthotropic materials, cohesive behavior, and favorable fracture planes. In recent years, several publications addressed these issues. In [3], an additional phase field was added to the original formulation. This allows for distinguishing different failure modes like matrix or fiber failure in composite materials. In [8,15,34], the so-called structural tensor was introduced, which accounts for favorable fracture planes by scaling the spatial gradient of the phase field. Failure in composite materials was considered by multiple researchers; actively

[11] Sebastian Pech, Vienna University of Technology (TU Wien), Austria, sebastian.pech@tuwien.ac.at
[2] Markus Lukacevic, Vienna University of Technology (TU Wien), Austria, markus.lukacevic@tuwien.ac.at
[3] Josef Füssl, Vienna University of Technology (TU Wien), Austria, josef.fuessl@tuwien.ac.at

https://doi.org/10.52202/069179-0053

pursued approaches are comprehensively summarized in [6,40]. Research regarding the use of the phase field method for wood was performed in [7] on the microscopic scale, in [33] on the macroscopic scale by incorporation of a representative crack element theory and in [27,28] by a hybrid macroscopic multi-phase field model based on the unified phase field theory. This work focuses on a discussion of the model developed in the latter works.

2 FUNDAMENTALS AND METHODS

Figure 1 shows the approximation of a sharp crack Γ with multiple diffuse representations $\Gamma_i(d_i)$ on a body Ω with the boundary $\partial\Omega$. The model from [27], a hybrid multi-phase field model for orthotropic materials with favorable fracture planes, is based on the unified phase field theory [39]. This adds a cohesive zones model to the formulation to account for effects like micro-cracking and fiber-bridging [31]. As the fracture behavior of wood is highly direction-depended, multiple phase fields [3] are used for cracks perpendicular to the longitudinal, radial and tangential direction.

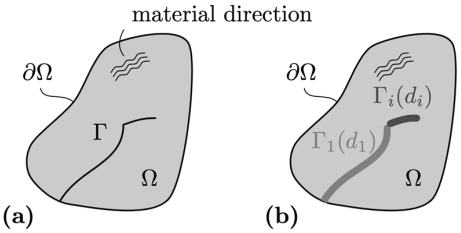

Figure 1: *Sharp and diffuse crack representation*

Excluding body forces and surface tractions, the regularized form of the total energy Π of the system, defined on the domain Ω, reads:

$$\Pi(\mathbf{u},\mathbf{d}) = \int_\Omega \left[\, \psi^+(\boldsymbol{u},\boldsymbol{d}) + \psi^-(\boldsymbol{u})\right] dV + \sum_{i\in\{L,R,T\}} G_{c,i} \int_\Omega \gamma_i(d_i)\, dV, \tag{1}$$

where i denotes the i-th phase field, $\boldsymbol{u}$ the displacement field, $\boldsymbol{d}$ the phase field of dimension 3 and $G_{c,i}$ the critical energy release rate. The strain energy terms $\psi^+(\boldsymbol{u},\boldsymbol{d})$ and $\psi^-(\boldsymbol{u})$ denote the degraded energy and undegraded energy, respectively. The crack geometry is approximated by the volume integral over the crack surface density function $\gamma_i(d_i)$. In the unified phase field theory, $\gamma_i(d_i)$, extended to include the structural tensor, is defined as

$$\gamma_i(d_i) = \frac{1}{c_{0,i}}\left(\frac{1}{l_i}\alpha_i(d_i) + l_i \nabla d_i \boldsymbol{A_i} \nabla d_i\right), \tag{2}$$

with $c_{0,i} = 4\int_0^1 \sqrt{\alpha_i(\beta)}d\beta$, $\alpha_i(d_i) = 2\,d_i - d_i^2$ as the local part of the dissipated fracture energy, and $\boldsymbol{A}_i = \boldsymbol{I} + \beta_i\,(\boldsymbol{I} - \boldsymbol{a}_i \otimes \boldsymbol{a}_i)$ as the structural tensor, where $\boldsymbol{a}_i$ is the material direction and β_i is the scaling factor of the structural tensor for phase field i.

Crack propagation is driven by an energetic force $\psi^+(\boldsymbol{u})$, which also dictates the constitutive behavior through the degraded strain energy $\psi^+(\boldsymbol{u},\boldsymbol{d})$. The phase field model described in [27] uses a stress-based split [32] to decompose the strain energy density into two parts: one that drives cracks and one that is inactive. The crack driving strain energy density is defined based on fracture mechanics failure modes I, II, and III for a crack perpendicular to $\boldsymbol{a}_i$. This includes the assumption that cracks mainly propagate following the principal material directions, which is motivated by the commonly observed "zig-zag" failure pattern of wood shown in Figure 2.

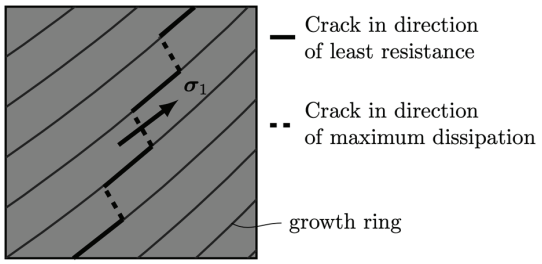

Figure 2: *Typical crack pattern of wood [31]*

The crack driving stress $\boldsymbol{\sigma}^+$ can be determined by projecting the undamaged stress tensor $\boldsymbol{\sigma}$ onto a fictitious crack surface with the crack normal vector $\boldsymbol{a}_i$ [16,27,32]. Subsequently, the mode I, II and III stresses are identified, allowing computation of $\psi_i^+(\boldsymbol{u})$. The crack orientation i that results in the largest energy release, indicated by the largest $\psi_i^+(\boldsymbol{u})$, defines the driving failure mechanism. As a result, Equation (1) is modified by replacing the original strain energy terms by

$$\begin{aligned}\psi_i^+(\boldsymbol{u},\boldsymbol{d}) &= \omega_i(d_i)\,\psi_i^+(\boldsymbol{u}) \text{ and}\\ \psi_i^-(\boldsymbol{u},\boldsymbol{d}) &= \psi_i(\boldsymbol{u}) - \psi_i^+(\boldsymbol{u}).\end{aligned} \tag{3}$$

Cohesive behavior is introduced by tuning the coefficients in the degradation function $\omega_i(d_i)$ and the crack surface density function $\gamma_i(d_i)$ on a one-dimensional bar problem with a single crack and a linear softening law [39].
The resulting energy minimization problem is solved with a staggered algorithm [4,22]. In addition, a hybrid approach [1] is used for degradation. This improves the solver's performance by making the deformation problem linear and, as shown in [27] and further outlined in Section 3.1, is required for adequately modeling the "zig-zag" crack pattern of wood. To prevent the interpenetration of crack faces, the hybrid approach is coupled with a smooth traction-free crack boundary condition [16]. Irreversibility of the phase field is enforced globally by an active-set reduced-space method [41]. An adaptive load increment scheme is adopted for further performance improvement which uses a trial point checker and a step size controller [14], restricting the increment size close to sudden changes in the dissipated energy and maintaining large increments during the linear elastic loading phase. The trial point checker performs an additional, however, very small load step, after a converged solution for the problem was found, and rejects

https://doi.org/10.52202/069179-0053

the converged state if the small additional step resulted in a change in the sign of the strain energy's slope. The step size controller works independently of the trial pointer checker an assures that after a failed load increment, the increment's size is reduced only as much as necessary to meet the convergence criterion.
The entire code is implemented in Julia [2]. For automatically deriving the element stiffness matrices and residual vectors from the energy formulation, the ForwardDiff-Package [30] is used. Pardiso 6.0 [10,18,36] is employed as the sparse linear solver.

3 RESULTS

3.1 VERIFICATION OF THE PHASE FIELD MODEL FOR WOOD

Initially, the described phase field model was verified on single-edge notched plates with varying fiber inclines and a more advanced example of a single knot in a wooden board with spatially varying principal material directions [27].
Figure 3 shows the edge notched plate under tensile loading by prescribing the vertical displacement at the upper edge. The fiber incline rises from 0 to 90 degrees. Initially, the crack path follows the weak interface between the growth rings. In a transition zone, the commonly found "zig-zag" pattern is recovered, and ultimately, the specimen fails with a crack perpendicular to the fiber direction.

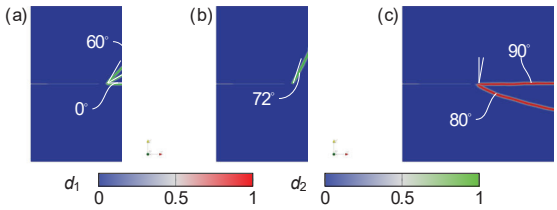

Figure 3: *Transition of failure modes from parallel to perpendicular to the fiber.*

Accurate reproduction of the "zig-zag" pattern in Figure 3 (b) requires applying the hybrid approach. This is related to the stress-based decomposition of the strain energy density described in Section 2. For forming the d_1 crack in Figure 3 (b), an energy state is required with substantial mode I, II and III stresses for the fictitious crack face defined by the normal vector in the longitudinal direction. Figure 4 shows a comparison of the longitudinal stress (i.e., the mode I stress for the d_1 crack) right before the failure of the specimen. Equation (3) is directly used to derive the constitutive relation in the variationally consistent approach. Therefore, the longitudinal stress is not degraded and, thus, peaks at the initial notch, reducing the crack driving energy at the diffuse crack tip for crack d_1. In comparison, in the case of the hybrid approach, everything except compressive mode I stresses is degraded. Therefore, the stress peaks at the diffuse crack tip, thus, allowing propagation of a $d_1$crack.

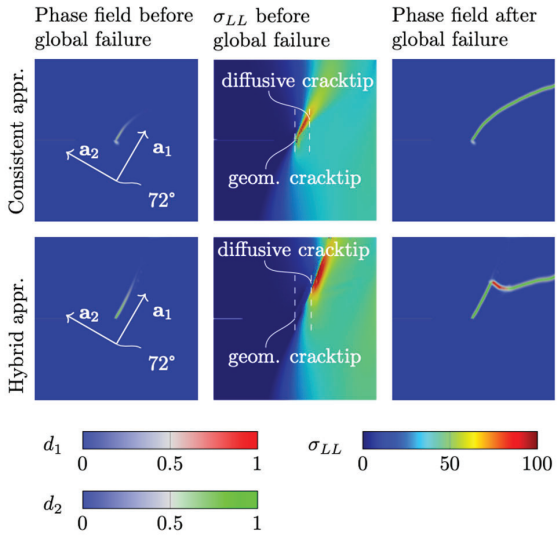

Figure 4: *Comparison of the hybrid and the consistent approach before the specimen's complete failure.*

Subsequently, the phase field model was tested on a more elaborate example. Figure 5 shows a wooden board with a single knot. The board is loaded at the bottom left edge, such that the initial crack is under tensile loading. The spatial fiber course is computed in each integration point using the model from [20]. As expected, the crack follows the fiber direction along the weak interface and shifts downwards in the vicinity of the knot until the whole specimen is cracked.

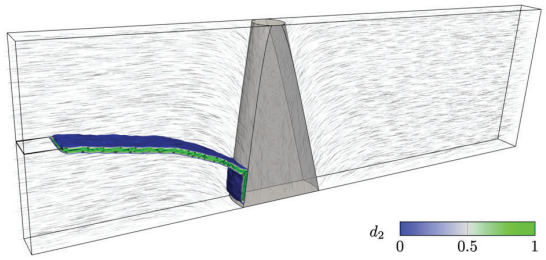

Figure 5: *Phase field crack in a wooden board with a single knot and spatially varying fiber courses.*

The results show that the hybrid multi-phase field model for wood can reproduce commonly found crack patterns of wood. Thus, it can account for the macroscopic structural effects influenced by the wood microstructure. Next, the model was validated on experimental setups in [28].

3.2 VALIDATION OF THE PHASE FIELD MODEL FOR WOOD

Three different types of tests were considered: A single edge-notched beam (SENB) [9,11], a double cantilever beam (DCB) [25] and an end-notched beam (ENB) [29]. Both the SENB and the DCB setups test for mode I

https://doi.org/10.52202/069179-0053

fracture properties; the ENB setup tests for mode II fracture properties.

In Equation (2), the structural tensor $\boldsymbol{A}_i$ is introduced in the formulation of the crack surface density function. The related scale factor β_i is an unknown quantity for wood and defines the intensity of the penalty constraint for invalid crack propagation directions. Due to the configuration of the SENB and the DCB test, β_i does not affect the crack orientation. However, the ENB test is strongly influenced by this quantity. Figure 6 shows the effect of increasing the scale factor for the primary driving failure mode in this test from 0 (isotropic formulation) to 90. This simulation allowed finding a lower bound of the structural tensors scale factor for wood. A value of 70 adequately reproduces the horizontal crack observed in the experiments in [29] and reduces the influence on the maximum load.

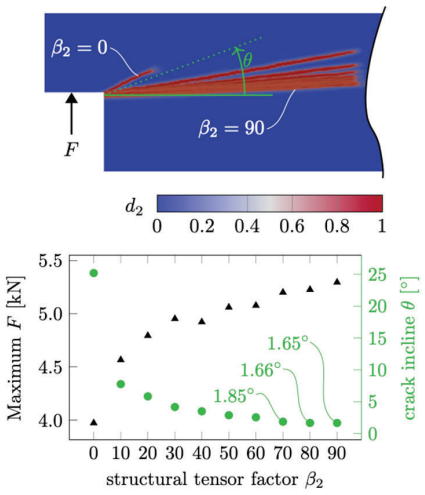

Figure 6: *Influence of the structural tensor's scale factor on the crack orientation and the ultimate load in the ENB test.*

Next, the SENB tests were simulated using the structural tensor scale factor value found for the ENB tests. Figure 7 shows the results for the tests in [9]. Using a multi-phase field model, it was possible to reproduce the experimental data very well with just a single model configuration (tensile strength and fracture energy release rate for L, R and T). Remarkably, the substantial difference in the ultimate load for a crack in the RL-plane and a crack in the TL-plane, also shown in [21], could be captured very well. Figure 8 shows the ultimate crack phase field for the SENB test in the RL-plane.

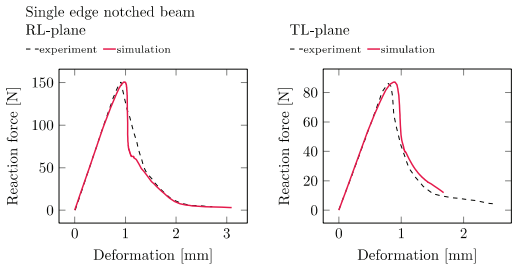

Figure 7: *Simulation and experimental graph of two SENB tests [9] with differently oriented failure planes (crack in RL-plane or TL-plane)*

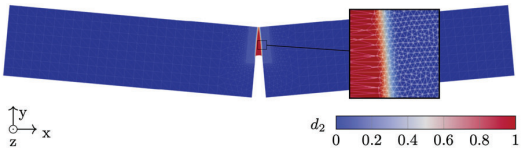

Figure 8: *Fully cracked SENB specimen for the setup from [9] in the RL-plane*

Subsequently, the model was tested on the DCB tests from [25]. Figure 9 shows a large scatter of the experimental data already in the linear elastic range. This was accounted for in the model by performing simulations for different scale factors of the elastic stiffness from 0.6 to 1.0. Keeping the tensile strength and the fracture energy release constant allowed the reproduction of the experimental data very well. To reduce the computational effort, only the region right after the initial notch was finely discretized. The crack in Figure 10 was sufficient to reproduce a substantial part of the experimental data in Figure 9.

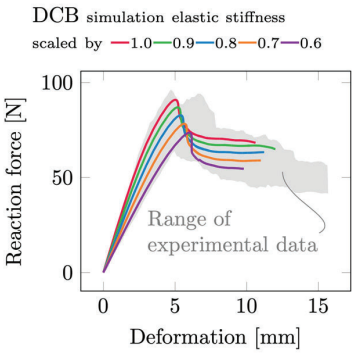

Figure 9: *Simulation and experimental results of a DCB test [25].*

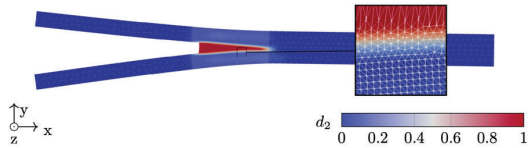

Figure 10: *Cracked DCB specimen*

Finally, the model was validated on the ENB test, which was already used to tune the scale factor of the structural tensor. In addition to a model with a tuned parameter configuration for this specific test, the material parameter found for the SENB tests of [9] were also used in the ENB model. The simulation and experimental results are shown in Figure 11. For both parameter sets, the response was within the experimental results.

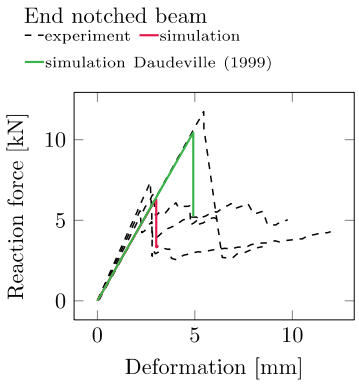

Figure 11: *Simulation and experimental results of the ENB test [29] for tuned model parameters and parameters from the SENB test from [9]*

The validation results in [28] show that the model is very well capable of reproducing experimental results, with the defining material properties, the tensile strength and the fracture energy release rate, well in a range known for wood. Furthermore, a lower bound for the structural tensor's scale factor was found, allowing the reproduction of the horizontal crack in the ENB test.
The phase field model presents a significant advantage over other models commonly used for simulating such experimental studies. Unlike in those models, the crack paths are not predefined. Instead, the model considers the local crack-driving energies and non-local effects induced by the microstructure of wood to form cracks. This approach makes the phase field model more adaptable and suitable for complex situations where the crack path is unknown in advance.

4 CONCLUSION AND SUMMARY

The present work describes implementing, validating, and verifying a phase field model for orthotropic non-brittle fracture of materials with favorable fracture planes and multiple, different failure mechanisms. The model is solved using a generally applicable staggered algorithm with globally enforced irreversibility constraints and an efficient load-stepping scheme. Using this model, it is possible to reproduce commonly found crack patterns of wood and the results of experimental tests. The model's input parameters, the tensile strength, and the fracture energy release rate are for all investigated tests within the range known for wood. Furthermore, values tuned to one experimental setup could be transferred to another setup with a different geometry. This suggests that the input parameters are material-specific rather than model-specific numerical parameters.
Compared to other three-dimensional finite element fracture mechanics simulation frameworks, the main advantage of the phase field method is that cracks of arbitrary complexity can be modeled. This is a fundamental requirement when simulating more complex wooden specimens like knot groups with spatially strongly varying fiber orientations. This work constitutes an important step towards the simulation of such complex models, which allow improved prediction of the load-bearing capacity of wooden boards. Based on an exact simulation using geometrical reconstructions of wooden boards with knots [17], homogenization procedures allow deriving metamodels similar to those in [21]. Such a simplified model allows the application to larger-scale structures or tasks, e.g., for the failure prediction of GTL beams [37], size-effect studies in GLT beams [38] or optimization of GLT beams [26].

ACKNOWLEDGEMENT

This research was funded in whole, or in part, by the Austrian Science Fund (FWF) Y1093-N30. The authors also acknowledge gratefully the support by the ForestValue project InnoCrossLam.

REFERENCES

[1] M. Ambati, T. Gerasimov, L.D. Lorenzis, A review on phase-field models of brittle fracture and a new fast hybrid formulation, Comput. Mech. 55 (2014) 383–405.
[2] J. Bezanson, A. Edelman, S. Karpinski, V.B. Shah, Julia: A fresh approach to numerical computing, SIAM Rev. 59 (2017) 65–98.
[3] J. Bleyer, R. Alessi, Phase-field modeling of anisotropic brittle fracture including several damage mechanisms, Comput. Methods Appl. Mech. Eng. 336 (2018) 213–236.
[4] B. Bourdin, G.A. Francfort, J.-J. Marigo, Numerical experiments in revisited brittle fracture, Journal of the Mechanics and Physics of Solids. 48 (2000) 797–826.
[5] B. Bourdin, G.A. Francfort, J.-J. Marigo, The variational approach to fracture, Springer-Verlag GmbH, 2008.
[6] T.Q. Bui, X. Hu, A review of phase-field models, fundamentals and their applications to composite laminates, Engineering Fracture Mechanics. 248 (2021) 107705.
[7] J. Carlsson, P. Isaksson, Simulating fracture in a wood microstructure using a high-resolution dynamic phase field model, Engineering Fracture Mechanics. 232 (2020) 107030.
[8] J.D. Clayton, J. Knap, Phase field modeling of directional fracture in anisotropic polycrystals, Computational Materials Science. 98 (2015) 158–169.
[9] L. Daudeville, Fracture in spruce: experiment and numerical analysis by linear and non linear fracture mechanics, Holz Als Roh-Und Werkstoff. 57 (1999) 425–432.

https://doi.org/10.52202/069179-0053

[10] A. De Coninck, B. De Baets, D. Kourounis, F. Verbosio, O. Schenk, S. Maenhout, J. Fostier, Needles: Toward Large-Scale Genomic Prediction with Marker-by-Environment Interaction, Genetics. 203 (2016) 543–555.
[11] N. Dourado, S. Morel, M.F.S.F. de Moura, G. Valentin, J. Morais, Comparison of fracture properties of two wood species through cohesive crack simulations, Composites Part A: Applied Science and Manufacturing. 39 (2008) 415–427.
[12] G.A. Francfort, J.-J. Marigo, Revisiting brittle fracture as an energy minimization problem, Journal of the Mechanics and Physics of Solids. 46 (1998) 1319–1342.
[13] A.A. Griffith, G.I. Taylor, VI. The phenomena of rupture and flow in solids, Philosophical Transactions of the Royal Society of London. Series A, Containing Papers of a Mathematical or Physical Character. 221 (1921) 163–198.
[14] A. Gupta, U.M. Krishnan, R. Chowdhury, A. Chakrabarti, An auto-adaptive sub-stepping algorithm for phase-field modeling of brittle fracture, Theoretical and Applied Fracture Mechanics. 108 (2020) 102622.
[15] V. Hakim, A. Karma, Crack Path Prediction in Anisotropic Brittle Materials, Phys. Rev. Lett. 95 (2005) 235501.
[16] T. Hu, J. Guilleminot, J.E. Dolbow, A phase-field model of fracture with frictionless contact and random fracture properties: Application to thin-film fracture and soil desiccation, Computer Methods in Applied Mechanics and Engineering. 368 (2020) 113106.
[17] G. Kandler, M. Lukacevic, J. Füssl, An algorithm for the geometric reconstruction of knots within timber boards based on fibre angle measurements, Constr. and Build. Mater. 124 (2016) 945–960.
[18] D. Kourounis, A. Fuchs, O. Schenk, Toward the Next Generation of Multiperiod Optimal Power Flow Solvers, IEEE Transactions on Power Systems. 33 (2018) 4005–4014.
[19] M. Li, J. Füssl, M. Lukacevic, J. Eberhardsteiner, C. Martin, Strength predictions of clear wood at multiple scales using numerical limit analysis approaches, Computers & Structures. 196 (2018) 200–216.
[20] M. Lukacevic, G. Kandler, M. Hu, A. Olsson, J. Füssl, A 3D model for knots and related fiber deviations in sawn timber for prediction of mechanical properties of boards, Materials & Design. 166 (2019) 107617.
[21] M. Lukacevic, W. Lederer, J. Füssl, A microstructure-based multisurface failure criterion for the description of brittle and ductile failure mechanisms of clear-wood, Engineering Fracture Mechanics. 176 (2017) 83–99.
[22] C. Miehe, M. Hofacker, F. Welschinger, A phase field model for rate-independent crack propagation: Robust algorithmic implementation based on operator splits, Comput. Methods Appl. Mech. Eng. 199 (2010) 2765–2778.
[23] C. Miehe, F. Welschinger, M. Hofacker, Thermodynamically consistent phase-field models of fracture: Variational principles and multi-field FE implementations, Int. J. Numer. Methods Eng. 83 (2010) 1273–1311.
[24] N. Moës, T. Belytschko, Extended finite element method for cohesive crack growth, Engineering Fracture Mechanics. 69 (2002) 813–833.
[25] M.F.S.F. de Moura, J.J.L. Morais, N. Dourado, A new data reduction scheme for mode I wood fracture characterization using the double cantilever beam test, Engineering Fracture Mechanics. 75 (2008) 3852–3865.
[26] S. Pech, G. Kandler, M. Lukacevic, J. Füssl, Metamodel assisted optimization of glued laminated timber beams by using metaheuristic algorithms, Eng. Appl. Artif. Intell. 79 (2019) 129–141.
[27] S. Pech, M. Lukacevic, J. Füssl, A hybrid multi-phase field model to describe cohesive failure in orthotropic materials, assessed by modeling failure mechanisms in wood, Engineering Fracture Mechanics. 271 (2022) 108591.
[28] S. Pech, M. Lukacevic, J. Füssl, Validation of a hybrid multi-phase field model for fracture of wood, Engineering Fracture Mechanics. 275 (2022) 108819.
[29] K. Rautenstrauch, B. Franke, S. Franke, K. Schober, A new design approach for end-notched beams: View in code, in: Paper No. CIB-W18/41-6-2, Proc., Meeting, 2008.
[30] J. Revels, M. Lubin, T. Papamarkou, Forward-Mode Automatic Differentiation in Julia, ArXiv:1607.07892 [Cs]. (2016).
[31] I. Smith, E. Landis, M. Gong, Fracture and fatigue in wood, J. Wiley, Chichester, West Sussex, England ; Hoboken, NJ, 2003.
[32] C. Steinke, M. Kaliske, A phase-field crack model based on directional stress decomposition, Comput. Mech. (2018) 1019--1046.
[33] D. Supriatna, B. Yin, D. Konopka, M. Kaliske, An anisotropic phase-field approach accounting for mixed fracture modes in wood structures within the Representative Crack Element framework, Engineering Fracture Mechanics. 269 (2022) 108514.
[34] S. Teichtmeister, D. Kienle, F. Aldakheel, M.-A. Keip, Phase field modeling of fracture in anisotropic brittle solids, Int. J. Non Linear Mech. 97 (2017) 1–21.
[35] S. Vasic, I. Smith, E. Landis, Fracture zone characterization - Micro-mechanical study, Wood and Fiber Science. 34 (2002) 42–56.
[36] F. Verbosio, A. De Coninck, D. Kourounis, O. Schenk, Enhancing the scalability of selected inversion factorization algorithms in genomic prediction, Journal of Computational Science. 22 (2017) 99–108.
[37] C. Vida, M. Lukacevic, J. Eberhardsteiner, J. Füssl, Modeling approach to estimate the bending strength and failure mechanisms of glued laminated timber beams, Engineering Structures. 255 (2022) 113862.
[38] C. Vida, M. Lukacevic, G. Hochreiner, J. Füssl, Size effect on bending strength of glued laminated timber predicted by a numerical simulation concept including discrete cracking, Materials & Design. 225 (2023) 111550.

[39] J.-Y. Wu, A unified phase-field theory for the mechanics of damage and quasi-brittle failure, J. Mech. Phys. Solids. 103 (2017) 72–99.
[40] J.-Y. Wu, V.P. Nguyen, C.T. Nguyen, D. Sutula, S. Sinaie, S.P.A. Bordas, Phase-field modeling of fracture, in: Advances in Applied Mechanics, Elsevier, 2020: pp. 1–183.
[41] H. Yang, C. Yang, S. Sun, Active-set reduced-space methods with nonlinear elimination for two-phase flow problems in porous media, SIAM J. Sci. Comput. 38 (2016) B593–B618.

https://doi.org/10.52202/069179-0053